CrossMark

TECHNICAL ARTICLE

Environmentally Hazardous Boron in Gold Mine Tailings, Timmins, Ontario, Canada

Cory C. Paliewicz · Mona-Liza C. Sirbescu ·
Thomas Sulatycky · Edmond H. van Hees

Abstract Traditionally, cyanide, mercury, and acid mine drainage are considered critical environmental hazards associated with gold mining. To our knowledge, this is the first study of hazardous concentrations of soluble boron (B) in a gold mine impoundment tailings dam. We suggest that the B anomaly is a consequence of disposal of gold pyrometallurgical waste (slag). Borax is a common flux used during fire assaying and refining of precious metals. Vast amounts of B-rich slag may have been discarded by mining operations and precious metal refineries worldwide, but the extent and effects of B contamination have not yet been addressed. Anomalous concentrations of soluble B found in the McIntyre mine tailings, Timmins, Ontario highly exceed recommended thresholds for groundwater, freshwater, and soil leachates, and cannot be explained by natural sources alone. Boron is distributed heterogeneously within the tailings dam and correlates positively with the percentage of ≤ 38 μm grain-size fraction, indicating that adsorption onto silt–clay particles results in B build-up.

Ephemeral, efflorescent Mg-borate found along the dam embankment suggests an outflow of B along paths of high permeability. Leachability tests indicate that slags from gold-ore refineries and fire assaying labs release ≤ 12 wt% soluble B in only 24 h. This high leachability suggests that slag discarded on the tailings dam is the dominant source of observed B anomalies. Altered metabasalts with $<3,000$ mg/kg B may be a minor B source. Gangue minerals such as tourmaline, anhydrite, calcite, and siderite cannot account for the amount of soluble B found in the tailings.

Introduction

Although cyanide, mercury, or acid mine drainage are the principal environmental concerns in gold mining and processing (Norgate and Haque 2012), recent tailings monitoring and closure assessments also include more benign contaminants, such as boron (B), to comply with increasingly stringent health and environmental regulations. Boron, although harmless and necessary to the human body when present in small concentrations, has received increased attention by regulatory governmental organizations because of its widespread industrial, agricultural, and household uses. Borax and other borates are well-established fluxes used during fire assaying of ore or final refining of precious metals because of their high efficiency and low cost. Vast amounts of B-rich slag may have been discarded without recycling by mining operations and precious metal refineries, but the extent of consequent B

C. C. Paliewicz · M.-L. C. Sirbescu (✉)
Earth and Atmospheric Sciences, Central Michigan University,
Mount Pleasant, MI, USA
e-mail: sirbe1mc@cmich.edu

Present Address:
C. C. Paliewicz
Geological Sciences, New Mexico State University, Las Cruces,
NM, USA

T. Sulatycky
Goldcorp Canada Ltd, Porcupine Gold Mines, Timmins,
ON, Canada

E. H. van Hees
Department of Geology, Wayne State University, Detroit, MI,
USA

anomalies and environmental hazards have not been addressed prior to this study.

Here we examine a soluble B anomaly at the McIntyre impoundment tailings Dam No. 5 in Timmins, Ontario, where massive amounts of B-rich slag were crushed and discharged between 1985 and 1991. Our main objectives were to: (1) describe the distribution of soluble B at depth in the McIntyre tailings; (2) understand how tailings grain size and permeability relate to B enrichments and its flow from its source(s) into the environment; and (3) identify the main source(s) of B anomalies, whether natural or anthropogenic. The conclusions of this case study may impact other current or historic mining operations and gold refineries with similar metallurgical and waste discarding practices.

Background on Boron Geochemistry

The Geochemical Cycle of Boron

Boron is a one of the lightest and most mobile elements, with a tendency to form anionic complexes because of its high ionization potential. The upper continental crust is highly enriched in B (17 mg/kg) relative to the primitive mantle (0.6 mg/kg) and bulk silicate Earth (0.3 mg/kg; Annovitz and Grew 1996; Leeman and Sisson 1996; McDonough and Sun 1995). Processes that dominate the B geochemical cycle in the crust include: (1) concentration in residual melts and incorporation in stable borosilicates, such as tourmaline; (2) transfer from igneous to surficial environments through volcanic exhalations; and (3) chemical and mechanical concentration in surficial environments (Leeman and Sisson 1996; Watanabe 1975). In addition, B abundance in rocks can change greatly as a consequence of rock-fluid interaction. For example, modern unaltered submarine basalts contain, on average, 5 mg/kg B, whereas basalts altered by seawater have B concentrations of 13.2 mg/kg (Fyon and Crocket 1982). B is also enriched in certain hydrothermal ore deposits, including orogenic and mesothermal gold deposits (Slack and Trumbull 2011).

Boron is an essential constituent in diverse classes of minerals including boric acid (sassolite), borates (e.g. borax, ulexite, and kernite), silicoborates (e.g. howlite), and borosilicates (e.g. tourmaline, datolite, and danburite), in which it has either threefold or fourfold coordination with oxygen. B is incorporated as a trace element in clay minerals, which explains the relatively low B concentrations in seawater and marine evaporites. In contrast, evaporation and fractional crystallization in closed basins result in major B accumulations (Smith and Medrano 1996; Walker 1975).

Boron and B compounds have many uses, including ceramics, glasses, insulation and textiles fibers, medicine, detergents, micronutrients in fertilizers, and anodic fuel cells (Annovitz and Grew 1996; Figen and Pişkin 2010). Borax ($Na_2B_4O_7 \cdot 10H_2O$) has been used for thousands of years to make ceramic glazes and to flux precious metal-bearing ores. More than 90 % of B is extracted from Cenozoic continental borate deposits such as those in California's Mojave Desert and in Turkey, followed by pre-Cenozoic marine evaporites and metamorphic deposits (Smith and Medrano 1996).

Boron in the Environment

The aqueous chemistry of B is controlled by B concentration and pH. At neutral or slightly acidic conditions in natural waters and soils, B occurs as undissociated boric acid $B(OH)_3$, a weak Lewis acid with relatively high solubility in water. At higher pH, boric acid accepts OH^- to form borate ions $B(OH)_4^-$, whereas at high B concentrations, regardless of pH, polyborate species, such as $B_3O_3(OH)_4^-$ and $B_4O_5(OH)_4^-$, become important, in addition to boric acid and borate (Leeman and Sisson 1996; Shibli and Srebnik 2005). B is an essential micronutrient for plants, but the range between deficient and toxic concentrations is unusually small (Shibli and Srebnik 2005). The surrounding geology and, in some cases, wastewater discharges, control the B concentrations in ground and surface water. Preventive measures, tailings remediation, and water deboronation technologies (Dydo and Turek 2013; Wolska and Bryjak 2013) rely on an improved knowledge of sources of natural and anthropogenic soluble B associated with mining industries. Typical anthropogenic sources of B to the environment include industrial cleaning products, irrigation water, coal surface mining, and fly ash (Leeman and Sisson 1996; Shibli and Srebnik 2005). Elevated B contents in groundwater have been tied, at least in part, with slag deposited in industrial landfills (Senior and Sloto 2006; Yoshinaga et al. 2011). Although borax has been widely used in pyrometallurgical processes of precious metals (Bugbee 1981; Marsden and House 2006), to our knowledge, B leachability from slag has not been investigated systematically prior to this study. In contrast, coal fly ash from power plants has been found to release significant amounts of B (Hayashi et al. 2010; Iwashita et al. 2005; Narukawa et al. 2003).

Boron is a necessary nutrient for human health and is consumed in fruit, vegetables, and water. Worldwide concentrations of B in drinking water range from 0.01 to 15.0 mg/L, consistent with ranges observed for groundwater and surface water because B is not removed by conventional wastewater and drinking-water treatment methods (WHO 2009). Boron is poisonous when ingested in excessive amounts. Long-term exposure to elevated B is also a matter of concern (Health Canada 2012; USEPA

(US Environmental Protection Agency) 2008). Limitations of B concentrations in drinking water range from 5.0 mg/L in Canada and 2.4 mg/L in the European Union countries, to as low as 0.6 mg/L in Minnesota, United States (Health Canada 2012; USEPA 2008; WHO 2009). A dose of 9.6 mg of B per kg of body weight per day gives severe adverse health effects (USEPA 2008). Estimates for lethal doses of B by oral ingestion vary from 15–20 g in adults to as low as 2–3 g in infants (USEPA 2006).

A U.S. Geological Survey (USGS) investigation of groundwater wells in southeastern Pennsylvania found a maximum B concentration of 5.24 mg/L in groundwater at a "Superfund" site contaminated by a metal extraction plant (Senior and Sloto 2006). In contrast, groundwater sampled from McIntyre Mine Tailings Dam No. 5 contained potentially lethal B concentrations of 243 mg/L. Such high anomalous B concentrations are rare, such as 640 mg/L of B in surface waters associated with open-pit mining of the largest borate deposit in the world, in western Turkey (Gemici et al. 2008).

Study Area

The McIntyre Tailings Complex

The Hollinger-McIntyre-Coniaurum deposit is the largest gold deposit in Canada and produced several tailings complexes in the Porcupine-Timmins gold camp. The 2.15 km^2 McIntyre tailings complex resulted mainly from mining of $\approx$ 37,000,000 metric tons (t) of ore with a production of 304,757 kg (10,750,000 oz) of Au between 1912 and 1989 and 90,000 t of Cu from 1963 to 1982 (Stevens et al. 2013). The tailings are a mix of cyanide leach tailings (produced until 1931) and a combined flotation tailings—concentrate cyanide leach tailings (until 1989) that were generated by the McIntyre mill (AMEC 2005). The tailings materials are mainly mixtures of silt to clay-sized particles composed of a wide variety of crushed minerals (silicates, carbonates, sulfides, oxides, etc.). The McIntyre tailings have an alkaline character because carbonates are abundant in both the crushed host rock and mineralized veins (AMEC 2005; Jamieson 2011).

The McIntyre tailings complex consists of five interconnected impoundment dams (Fig. 1) located approximately 2.5 km east of the center of city of Timmins (population of about 43,000) and immediately north of Schumacher, a former town included when the City of Timmins was incorporated. The dams were built on a lacustrine plain with low-lying wetland and forested areas. Tailings were deposited as fine-grained sediment–water

slurry by spigotting along 150 m sections moved sequentially around the perimeter to ensure even filling of the basin. As a result, the McIntyre tailings deposits resemble overlapping alluvial fans in natural systems (Hudson-Edwards et al. 2011; Lottermoser 2010).

A geotechnical and environmental tailings closure assessment documented perimeter embankments as high as 30 m in height that were built of tailings using an upstream method to provide containment (AMEC 2005; Lottermoser 2010). The tailings complex lies between Clear Water Lake to the southeast and the Hersey Lake Conservation Area wetland to the north (Fig. 1). The surface drainage pattern of the McIntyre tailings coincides with the headwaters of the Porcupine River flowing east, which receives water that discharges from the McIntyre tailings as surface runoff, groundwater seepage, or decanted dam water (AMEC 2005). Groundwater mounding and radial flow towards surrounding surface water bodies are caused by localized infiltration of meteoric water in the center of the tailings complex (Fig. 1; AMEC 2005).

The McIntyre Mine Tailings Dam No. 5

Dam No. 5 occupies an area of 0.68 km^2, sloping gently towards its northern boundary with Dam No. 2. The west perimeter of Dam No. 5 is about 14 m in height, sloping towards and underlain by the older Hollinger Mine Tailings Dam in the southern segment and by 5 cm of thin peat and glacial/lacustrine sandy sediments in the central and northern segment (Fig. 1). Cumulatively, Dam No. 5 and Hollinger tailings deposits are 19–20 m thick on the southern margin. North of the Hollinger Mine Tailings Dam, the Dam No. 5 deposit thins out to only 7–8 m thick as intercepted in our borehole transect B (Fig. 1; Appendix 1). The southern, thicker segment of Dam 5 was visible on aerial photographs as early as 1949, whereas the central-northern, thinner portion is a more recent expansion of McIntyre Mine Tailings complex, beginning in 1981 (AMEC 2005). Reported water table contours (Fig. 1) suggest that localized groundwater flows towards the western and southwestern perimeter of Dam No. 5. According to groundwater contours in 2004, the water table was located at $\approx$ 8–7 m above the bottom of the tailings in the southern segment of Dam 5, and at 1 m above the bottom of tailings to below the tailings in the central and northern segments.

The AMEC (2005) closure assessment reported localized B anomalies in bulk surface samples collected at Tailings Dam No. 5 (up to 952 mg/kg), soil leachate (up to 57.7 mg/L), local groundwater (up to 242.0 mg/L in monitoring well GW1; Fig. 1), and locally discharged surface water (up to 9.1 mg/L near GW2; Fig. 1). Although animal and plant B tolerance levels are widely variable, the
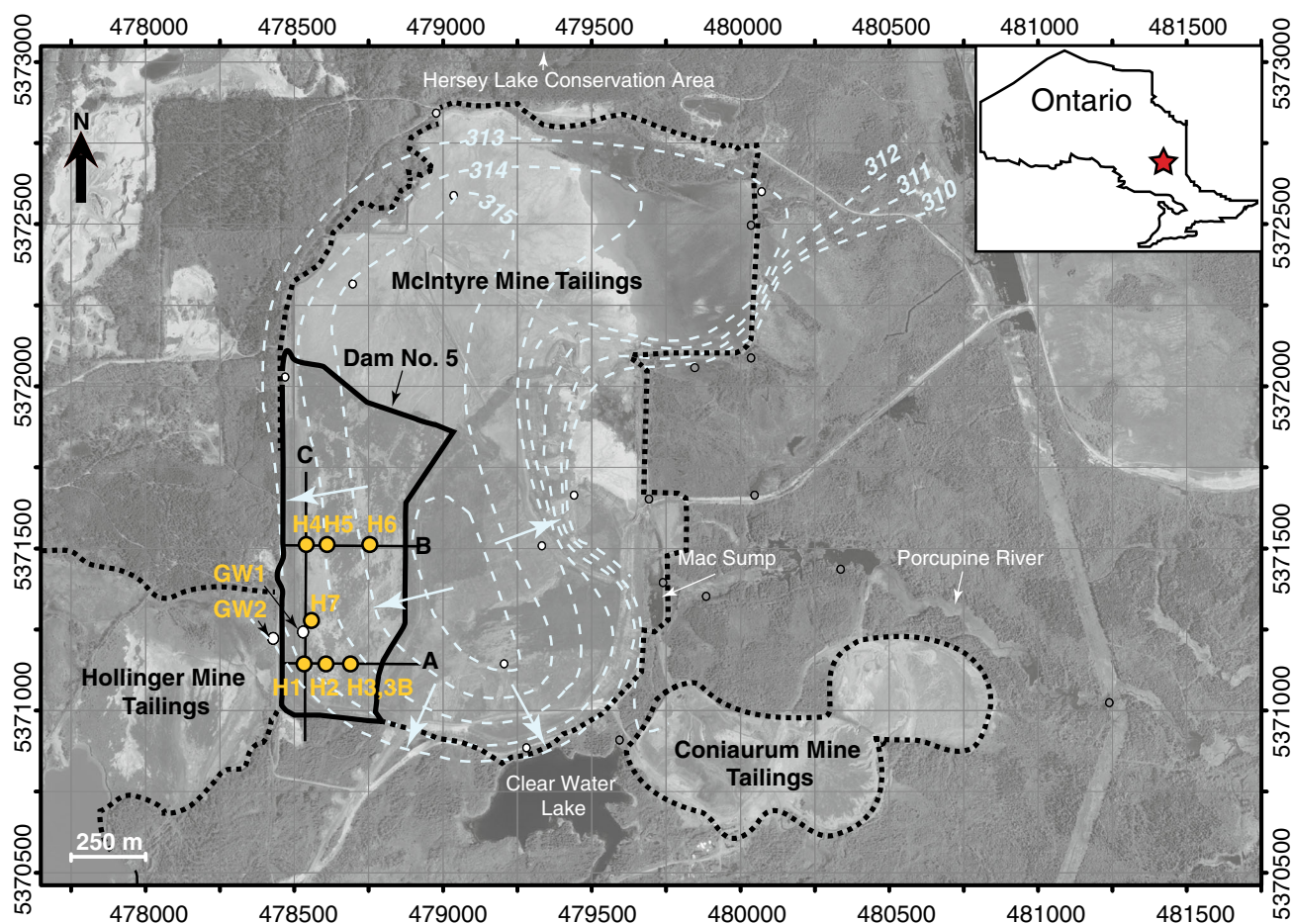
Fig. 1 Map of the McIntyre mine tailings dam showing borehole locations (H1 to H7) and sampled groundwater wells GW1 and GW2 (identical to wells BHM0306 and BHM0307 in AMEC 2005). Geographic coordinate system: North American Datum 1983 (1989). *Small dots* represent locations of groundwater monitoring wells (*white*) and surface water samples (*gray*). The outlines of the McIntyre mine tailings (*dashed black line*), Dam No. 5 (*solid black line*), and 2004 groundwater contours and main flow lines in the study area (*dashed blue lines and arrows*) are after AMEC (2005); Ontario inset map shows the location of Timmins (*star*)

observed levels far exceed the recommended thresholds of 5–8 mg/L for soil leachate (Nable et al. 1997) and 0.75–1.0 mg/L for freshwater environments (Black et al. 1993; Cano-Reséndiz et al. 2011). The localized B contamination in Dam No. 5 of the McIntyre gold mine tailings is both an environmental problem and an enigmatic question of source.

Potential Natural Sources of Boron

Mesothermal gold mineralization in the Timmins–Porcupine gold camp was mined at some 25 locations, among which the most notable are Dome, Aunor-Delnite, Hollinger, McIntyre, Buffalo Ankerite, Pamour, Hoyle Pond, and Owl Creek mines. Currently, only Dome and Hoyle Pond are operational (Stevens et al. 2013). The gold deposits are quartz–pyrite–ankerite–anhydrite–albite–tourmaline veins and stockworks formed by metamorphic solution-remobilization in 2.65–2.75 Ga host rocks of the Porcupine-Destor deformation zone in the Abitibi Greenstone Belt subprovince, Archean Superior Craton (Bateman et al. 2005; Slack 1996). Like other mesothermal gold deposits, the Timmins–Porcupine gold mineralization is somewhat enriched in B (Guilbert and Park 2007; Payne 1992). Certain gangue minerals and/or hydrothermally altered host rocks of the gold ore could be a source of B contamination in the tailings if significant amounts of B were released as soluble B after ore processing and subsequent weathering.

Natural sources of B in the Timmins–Porcupine gold camp include weathering-resistant tourmaline (with 3.1–3.4 wt% B), more soluble gangue minerals such as carbonates or anhydrite ($CaSO_4$), and B-rich fluid inclusions trapped in gangue minerals. In addition, tholeiitic metabasalts have Mg-rich carbonate-alteration zones in the vicinity of Au mineralization, with average B

concentrations of 528 mg/kg and as high as 3,000 mg/kg, about 600 × greater than the B content of local non-mineralized metabasalts (Fyon and Crocket 1982).

Slag as a Potential Source of Boron

In the Timmins–Porcupine gold camp, a number of mining operations, including the McIntyre Mine, had associated refineries and fire assay labs that followed traditional ore smelting with a B-rich flux. Although the flux recipe is adjusted as a function of bulk rock composition, borax (or anhydrous borax) is usually a main ingredient (12–50 wt%; Bugbee 1981; Marsden and House 2006). Therefore, the resulting pyrometallurgical waste (slag) can be extremely rich in B.

The Pamour Porcupine Mine Manager's files indicate that McIntyre refinery slag was shipped to the Noranda Smelter in Noranda, Quebec for reprocessing, so it is highly unlikely that McIntyre gold refinery slag ended up in Tailings Dam No. 5 (Kent 1988). However, a 225 t/day custom milling circuit called the Timmins GoMill (Govt of Ontario Mill) operated as a separate circuit in the main McIntyre Mill from 1985 to 1991 (AMEC 2005). During this time, GoMill processed an estimated 60,000 t of slag and refinery bricks (75 % slag: 25 % brick) for a precious metal refinery, as well as gold ore from other mining operations in the gold camp (Pamour Porcupine Mine Manager Monthly Reports 1984–1991; Yeoman written communiqué). The B-fluxed slag and brick processed by GoMill were directly discharged into Dam No. 5 (Landers, Vos, and Yeoman, written communiqués). It is important to note that the 1985–1991 slag disposal overlapped with a period of expansion of the McIntyre Mine tailings complex responsible for the central-northern segments of Dam No. 5 starting in 1981 and continuing for 2 years after the McIntyre Mine was closed in 1989.

Methods

Sample Collection

Eight boreholes (labeled H1, H2, etc.) were drilled near the western edge of McIntyre Tailings Dam No. 5 with a hand auger (consisting of attachable 1.5 m steel rods) to a depth of ≤9.1 m, along three traverses (A, B, and C; Fig. 1). The location of traverses was selected in an area of anomalous B concentrations according to the previous environmental closure assessment (AMEC 2005). Traverses A (H1–H3B; 140.7 m long) and B (H4–H6; 186.9 m long) are perpendicular to the edge of the dam. Traverse C (H1–H4; 349 m long) is parallel to the edge of the dam and runs in a north–south direction (Fig. 1). Traverse A boreholes reached about 8–10 m above the bottom of the tailings dam (AMEC 2005) and did not intercept the groundwater table. Boreholes in traverse B penetrated through the unlined bottom of the tailings dam at a depth of ≈7–8 m and intersected the underlying organic-rich "paleosoil" (peat) and natural sand and gravel deposits, as well as the groundwater table (Appendix 1). Therefore, based on available records, the top 7–8 m of sediment investigated in this study were deposited between 1981 and 1991.

Tailings samples consisted of 0.3 m long cores collected at 0.45 m intervals. Continuous sampling was employed for better resolution near the area with the highest reported B (H3B) in H7, located near a ≈100 m long, ≈1–2 m wide, horizontal layer exposed at the surface along the edge of the dam (Fig. 2). The surface layer was covered with a highly soluble, powdery, white efflorescent mineral. The friable, <3 mm thick mineral encrustations were sampled for identification. Only traces of the surface efflorescent mineral were found 5 months after the initial collection and heavy rainfall, indicating the ephemeral nature of this mineral precipitate. Groundwater samples

Fig. 2 a View towards north of the western perimeter of the McIntyre Mine Tailings Dam No. 5 showing a 1–2 m thick layer of white efflorescent precipitate mineral; **b** close up image of the efflorescent mineral occurring as a white crust on tailings clumps
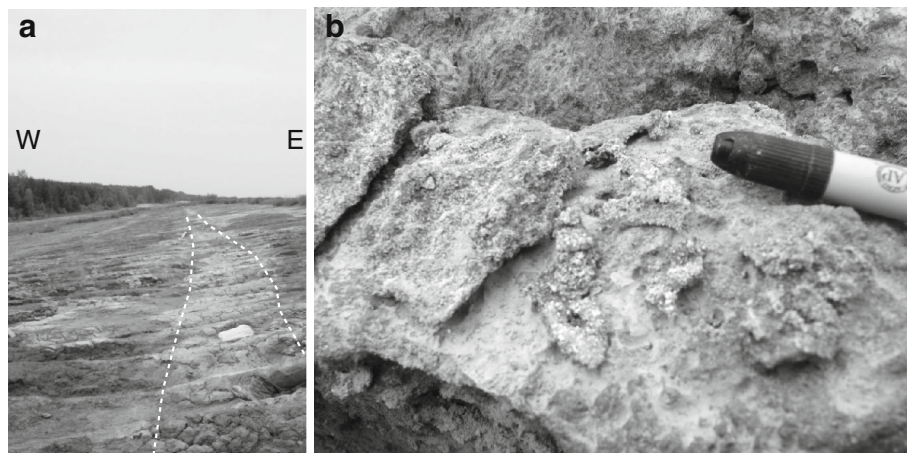
Table 1 Crush-leach results for slag samples acquired in 2012–2013 from three gold operations from the Timmins area

Slag no.	Gold operation	Slag source	Texture and color	B (wt%) leachable in water	pH of leachate
BP2	Dome	Assay Lab	Aphanitic, green	4.83	12.38
BP3	Dome	Refinery	Porphyritic, dark	11.84	11.66
BP4	Dome	Refinery	Porphyritic, dark	8.15	11.33
BP5	Dome	Refinery	Aphanitic, black	6.26	10.99
BP6	Bell Creek	Refinery	Aphanitic, green	3.92	12.39
BP10	Lake Shore	Refinery	Aphanitic, brown red, green	3.59	10.93
BP11	Lake Shore	Assay Lab	Aphanitic, light green	6.28	11.24

The amount of leachable boron (wt%) was calculated based on B concentration in the leachate solution after 24 h of flask-shake leaching in distilled-deionized water

from nearby water monitoring wells GW1 and GW2 were also collected (Fig. 1).

Seven slag samples (Table 1) produced by gold ore refining and fire assaying were obtained from the Dome, Lake Shore, and Bell Creek Mines in Timmins to test as potential sources of soluble B analogous to the 60,000 t of refinery slag and brick deposited in the McIntyre tailings dam during the late 1980s–early 1990s. Slag samples were light green to black. Five samples were aphanitic and composed entirely of glass. Two of the samples had a porphyritic texture, being composed of glass and up to 30 mm long acicular crystals (Table 1).

Preparation for Leachate Analysis

Prior to chemical analyses, the tailings samples were transferred to aluminum pans and placed in a convection oven to dry at 60 °C. Once dried, the samples were gently disaggregated with a mortar and pestle and homogenized using a stainless steel, gravity-fed Endecotts sample splitter. They were then quartered into four homogenized samples for various analyses. Slag samples were pulverized using a Sepor Inc. rock-grinding rotary mill for 20 s.

Leaching Tests

Dry, homogenized tailings samples were mixed with distilled deionized water (DDIW) in volumetric flasks using a solid to DDIW ratio of 1:3. These mixtures were then mechanically shaken for 24 h using a flask-shaking device. 50 ml of this slurry was centrifuged for 30 min in a Damon IEC Model HN–S II centrifuge at 1,600 rpm. The clear leachate was decanted and filtered for ion chromatography (IC) using 0.45 μm Fischer Scientific nylon filters 13 mm in diameter.

Pulverized slag samples were leached using the same 24 h flask-shaking method used for the tailings samples. A reduced slag to DDIW ratio of 1:5 instead of 1:3 was required to prevent saturation of leachate solutions. Prior to analysis by ICy, the slag leachates were diluted with DDIW by a factor of 10, to avoid exceeding the linear range of the conductivity detector of the IC. The B leachability of the crushed slag was tested following the same leaching procedure as for pure water, using leaching solutions with pHs ranging between 5 and 9. The leaching solutions were mixtures of dibasic sodium phosphate (Na_2HPO_4) + potassium biphthalate ($C_8H_5KO_4$) for pH $\approx$ 5; monobasic potassium phosphate (KH_2PO_4) + Na_2HPO_4 for pH $\approx$ 6 and pH $\approx$ 8; and $NaHCO_3$ + Na_2CO_3 for pH $\approx$ 9. To analyze the pH of slag leaching and leachate solutions, a Corning 240 pH meter was calibrated using three standard solutions of pH 4.00, 7.00, and 10.00 $\pm$ 0.02 at constant room temperature of 25 $\pm$ 1 °C prior to each set of analyses. The leaching solutions and resulting leachates were analyzed within 2 h of preparation and separation from the solids, respectively.

Ion Chromatography

Boron analysis was conducted using a Dionex D320 IC equipped with an LC25 chromatography thermostat and a conductivity detector and 9 × 250 mm Dionex IonPac ICE ion-exclusion borate separation column coupled with a 4 mm AMMS–ICE 300 Dionex anion micromembrane suppressor. The eluent solution was a mixture of 2.5 mM methanesulfonic acid and 60 mM mannitol and the regenerant solution was a mixture of 25 mM electronic grade tetramethylammonium hydroxide and 15 mM mannitol. The retention time for H_3BO_3 occurred at 7.9 $\pm$ 0.1 min, at an eluent flow rate of 0.85 ml/min. A constant pressure of 2.5 psi of nitrogen gas established a regenerant flow rate of $\approx$ 3 mL/min. Fisher Scientific reference solution SB155–100 and solid boric acid NIST–951 were used to produce the standards and validation solutions ranging from 1 to 250 mg/L B. The detection limit for B was estimated at 0.01 mg/L B; the average relative analytical error was 1.8 %.

Tailings Characterization

A series of sieves 7.6 cm in diameter was used for the grain size analysis of all 57 borehole samples from traverse A (about half of the tailings samples collected for this study). We used 250, 150, 106, 75, and 38 μm sieve sizes, corresponding to the U. S. Standard ASTM mesh values of 60, 100, 140, 200, and 400, respectively. To prevent flocculation, 25 g of dry sample were mixed with 75 mL of 25 g/L sodium hexametaphosphate solution. The mixture was flushed through the sieves with water. The fractions were collected in pre-weighed disposable sample dishes, dried in ≈60 °C oven overnight, weighed, and converted to grain size distribution (%) (Appendix 2).

The color of homogenized, uniformly wetted, tailings samples was characterized using standard Munsell soil color charts (Munsell® Color 2010) and recorded in Hue Value/Chroma format (Appendix 1). The color for each sample was copied and pasted from a digital version of the Munsell color system and displayed in Appendix 1.

Other Analyses

We used laser ablation—ion coupled plasma-mass spectrometry (LA–ICP–MS) to analyze the B contents of anhydrite from the McIntyre Mine (van Hees collection—mid 1980s), as the most common gangue non-silicate in the Cu-Au mineralization. One representative sample was mounted in epoxy, polished, and analyzed with an Element II mass spectrometer equipped with an Analyte193X Excimer laser system (Photon Machine Inc.). The ablation of 40 μm spots was optimized at a laser power output of 60 % and a frequency of 10 Hz (600 pulses/s). The stoichiometric value of 29.438 wt% Ca was used as internal standard of anhydrite. Two glass standards were used for calibration: NIST 612 (8.500 wt% Ca and 35 mg/kg B) and BCR2G (5.043 wt% Ca and 6 mg/kg B). Scanning electron microscopy—energy dispersive spectroscopy (SEM–EDS) qualitative compositional data and back scattered electron (BSE) images were collected on the efflorescent precipitates using a JEOL JSM–840A SEM. The accelerating voltage was 20 kV. Prior to the spectral analysis, the samples were mounted on double-sided sticky tape and gold-coated.

Results

Tailings Chemistry

Boron concentrations of tailings leachates and groundwater samples ranged from below analytical detection to 249 mg/L (Appendix 1). B concentrations and relative abundance (in wt%) of silt–clay fraction (≤38 μm) of tailings were plotted as a function of depth to better understand the B distribution in Dam No. 5 (Fig. 3). In general, there was good correlation between B and the silt–clay fraction (≤38 μm). The B concentrations (isopleths) were contoured on depth versus horizontal distance diagrams for traverses A through C using unsmoothed Delaunay triangulation software (Fig. 4).

Traverse A has a decreasing leachable B trend from boreholes H3 and H3B on the center of the dam, towards H1, near the edge of the dam (Fig. 4a). Boreholes H3 and H2 have very similar B distributions with depth that appear vertically offset by about 0.5–1 m. The distribution of B mimics the westward sloping groundwater table that is situated immediately below the sampled interval in traverse A. Traverse B has an opposite trend, with the highest B at the western edge of the dam (H4; Fig. 4b), whereas the center borehole (H5) contains the lowest B. Borehole H7 in traverse C (Figs. 1, 4c) is located 25 m east of the efflorescent-mineral occurrence along the western embankment of the tailings dam (Fig. 2). Little to no detectable B was found in H7. The small B enrichment at a depth of 1.5 m in H7 (Fig. 3) correlates to an approximate depth of ≈1.8 m below the top of the dam where the layer of Mg-borate crystals was found (Fig. 2). The second, larger "peak" in H7 (22.3 mg/L B) at a depth of 5.0 m (Fig. 3) appears to correlate with the maximum values of B measured in H1 (31.2 mg/L) and H4 (134.7 mg/L) at 6.4 m below surface (Figs. 3, 4c). Boron concentrations of two groundwater samples from monitoring wells GW1 and GW2 (Fig. 1) had 20.2 and 81.3 mg/L B, respectively, which are consistent with B concentrations in leachates from nearby boreholes H7 and H1 (Fig. 1; Appendix 1).

A scanning electron microscope (SEM) was used to study the morphology and chemical composition of the white efflorescent mineral precipitate, which consisted of ≈60 μm diameter clusters of pseudo-hexagonal, tabular micro-crystals ≈10 μm in diameter (Fig. 5a, b). A qualitative IC analysis of the mineral dissolved in ultra-pure water found that B was an essential constituent. An energy-dispersive spectrometry (EDS) analysis indicates that Mg and O were essential constituents of the microcrystals (Fig. 5c), but B is too light to be detected by EDS. The combined IC data and SEM–EDS spectra suggest that the mineral is a hydrous magnesium borate. LA–ICP–MS data collected on vein anhydrite collected from the McIntyre Mine (van Hees collection from mid 1980's) found only trace amounts of B, ranging from 4.12 to 5.27 mg/L of B (average 4.63 mg/L).

Sediment Characterization and Grain Size Distribution

Tailings sediment is mainly silt with variable proportions of clay and fine sand-sized particles, according to the USGS Wentworth grain size chart (Wentworth 1922;

Fig. 3 Boron in mg/L (*open circles*) and relative abundance in wt% of fraction ≤38 μm (*solid circles*) in tailings leachates as a function of depth

Boron (mg/L) and Grains <38 μm (wt%)
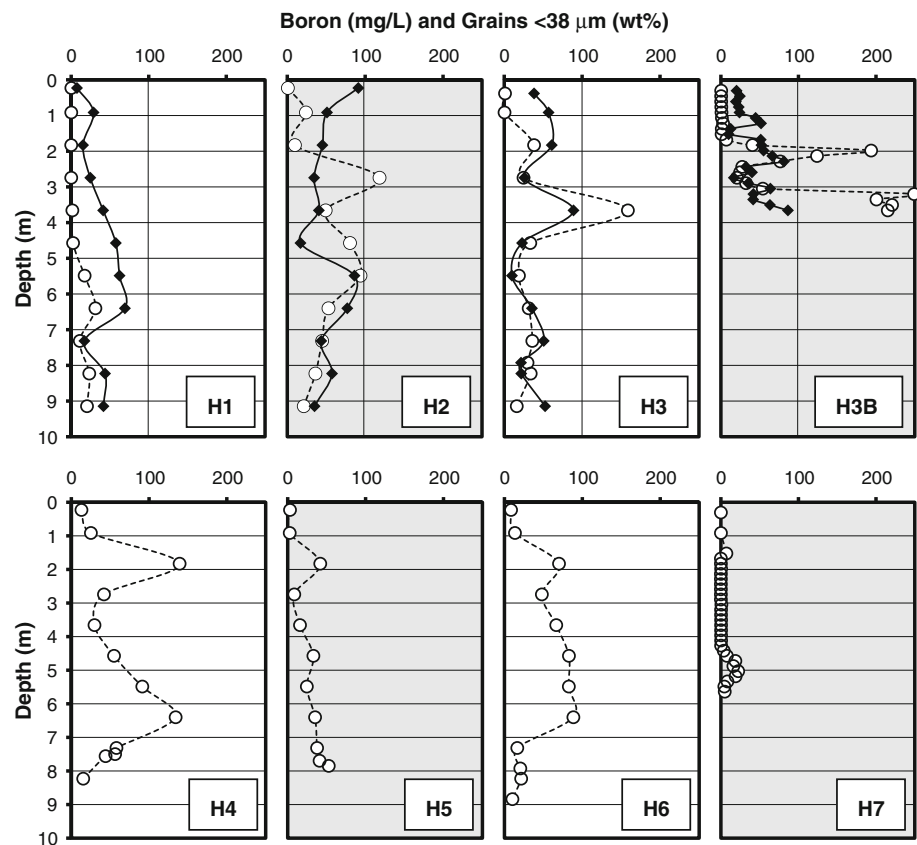
Williams et al. 2006). Color, grain-size estimates, and B content were recorded as a function of depth (Appendix 1). Coarser sediment (sand) was documented near the western edge of Dam No. 5, but grain size varied inconsistently with depth. Some borehole samples were heterogeneous, consisting of silty-sand material intercalated with thin intervals of clay. The initial water content of the samples varied from dry to moist to water-saturated when the water table or perched water tables were intersected. There was a noticeable transition from oxidized, light olive-brown or olive to reduced, gray or bluish-grey sediment at 1.5–1.8 m in all boreholes. Distinctly gray, dark gray, or dark bluish-grey clay-rich material appeared to yield leachates with the highest B concentrations (H3 and H3B, Appendix 1).

The weight percentages of the finest fraction (≤38 μm) from traverse A samples were plotted against depth and B concentrations (Figs. 3, 6). The first 1.8 m of boreholes H1—H3B had variable grain-size distributions and generally quite low B contents. A general positive correlation between B content and the relative amount of silt/clay-sized grains is apparent below a depth of 5.5 m in H1 and H2, and below 1.8 m in H3 and H3B (Figs. 3, 6). The exceptions to this linear correlation in H3B can be noted at depths ranging between 2.0–2.1 and 3.2–3.7 m with B concentrations that lack, or have a poor negative correlation with the wt% of the finest fraction (Fig. 6). Instead, at

these levels, there appears to be a distinct association between B contents with the color and texture of tailings sediment. For example, the H3B outliers that have B concentrations in excess of 200 mg/L are associated with dark gray lumps of clay (Appendix 1).

Chemistry of Slag Leachates

The B concentrations of slag leachates ranged between 6,954 and 19,664 mg/L of B, several orders of magnitude higher than the B contents of the tailings leachates. We define the B leachability of the slag as the weight percentage of soluble B relative to the initial mass of solid slag, measured in wt% rather than mg/L. The B leachability of the slag ranged from 3.6 to 11.8 wt% B in DDIW (Table 1). The leachability of aphanitic samples averaged 5.00 ± 1.3 wt% B (N = 5). Two partly crystallized slag samples (BP3 and BP4) released even more soluble B, amounting to 8.1 and 11.8 wt%, respectively.

A preliminary leaching study was conducted to test whether leachable B changes with the pH of the leaching solution. Leaching solutions ranging from pH 5 to 9 led to a nonsystematic, sample-dependent effect. The concentration change relative to leachates in DDIW ranged from −45 % to +13 % for an initial pH of ≈5 and ≈8, respectively. The final pH of all slag leachate solutions was
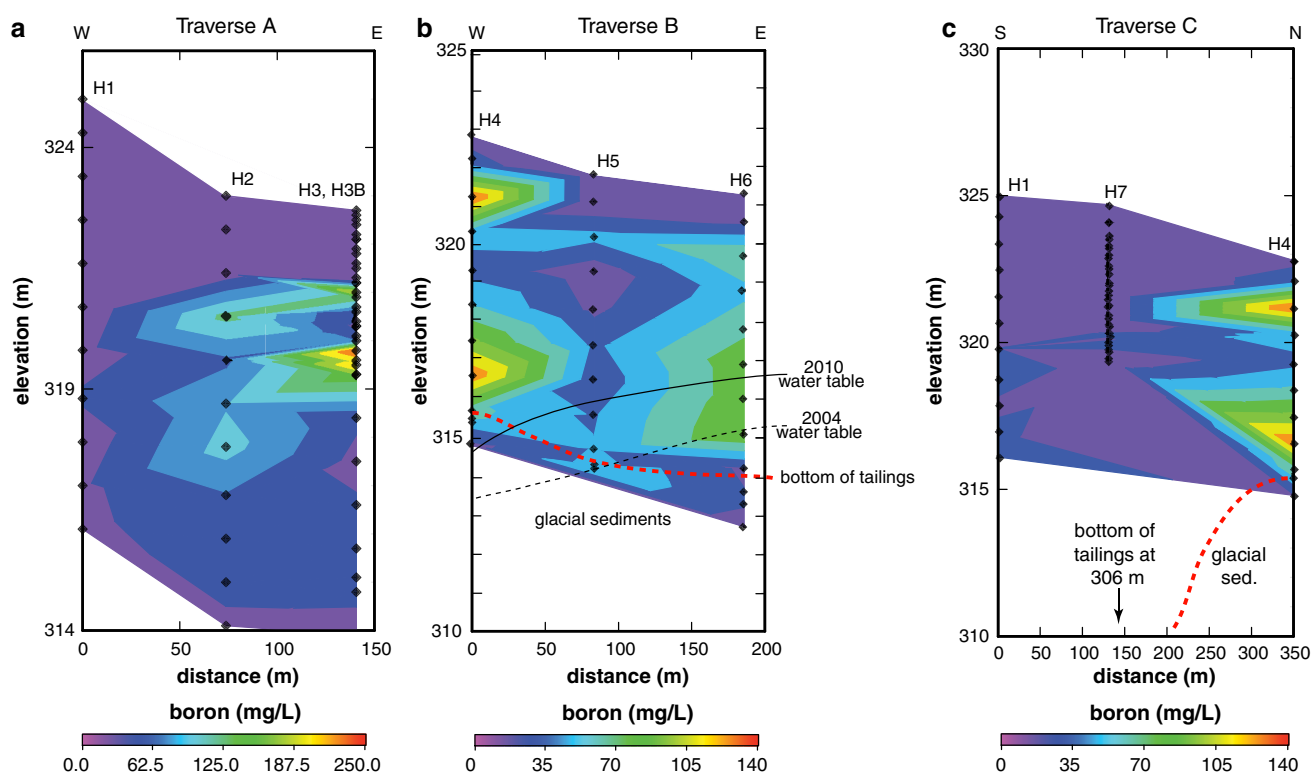
Fig. 4 Boron isopleths (in mg/L) for the three sampling traverses illustrated in Fig. 1: **a** traverse A perpendicular, **b** traverse B perpendicular, and **c** traverse C parallel to the western edge of McIntyre Dam 5, respectively

buffered by the soluble slag components to values between ≈ 11 and 13, regardless of the initial pH of the leaching solutions (Fig. 7a). The lower pH (10.3) of slag BP-5 leached with a carbonate-bicarbonate solution of initial pH of ≈ 9 correlates with an apparently lower B concentration (1.67 wt%), which was likely caused by saturation and precipitation of a B-rich phase.

There was a linear correlation between the B leachability of slag samples and the pH of the leachate solution (Fig. 7b), indicating that B speciation is the main pH buffer in these solutions. Two slag samples fall off this trend, at higher pH, suggesting that a different buffer, in addition to B species was likely involved (carbonate/bicarbonate ions), perhaps related to a different flux recipe used during gold extraction or because of slag heterogeneity. A more systematic study of slag leachability is needed, involving a larger number of representative slag samples.

Discussion

Spatial Distribution of Soluble Boron

Borehole data show that B anomalies are distributed heterogeneously within the 9 m or less at the top of Dam No. 5 (Figs. 3, 4). B concentrations of tailings leachates correlate weakly between nearby boreholes, suggesting some continuity of B-rich layers throughout the southwest segment of Dam No. 5 (Figs. 3, 4). The layered spatial distribution of soluble B can be controlled by primary and/or secondary factors. A primary control is the heterogeneous distribution of natural and anthropogenic B sources in the tailings. In contrast, secondary B enrichments are caused by hydrodynamic and sorption processes (both absorption and adsorption), in which soluble B is remobilized and redistributed by meteoric and groundwater flow from source location(s) within the tailings dam and concentrated in zones of low permeability. The secondary remobilization of B-rich fluids is likely confined to highly permeable well-sorted, coarse-grained zones.

Boron enrichments generally occur in, or directly above, less permeable layers, as indicated by the correlation between B and percent of silt/clay-sized sediments (Figs. 3, 6). Recent studies have found that B has high affinities for clays or clay-sized grains and that Mg is an important component for trapping B. For example, Goldberg and Suarez (2011) observed B adsorption on clays in soils increasing with the pH and Mg content. Dionisiou and Misopolinos (2006) demonstrated that MgO could be used as a B removal agent from irrigation waters. Tholeiitic basalts and gold-bearing mineralization containing ankerite $(Ca(Fe, Mg, Mn)(CO_3)_2)$ are common at the McIntyre

Fig. 5 White efflorescent Mg borate mineral collected on the surface of the McIntyre Dam 5 tailings (Fig. 2): **a** and **b** SEM images of clusters of pseudohexagonal, tabular microcrystals; **c** EDS spectrum showing the presence of Mg and oxygen

The heterogeneous B distribution at the western perimeter of Dam No. 5, as illustrated in transect C (Fig. 4c) may have been caused by: (1) B seepage from the H1-H7 segment located in close proximity to the Mg-borate layer; and (2) migration into and adsorption within two localized B-rich plumes that correspond with the dark gray and bluish-gray tailings sediments intercepted by H4 (Appendix 1). Alternatively, B enrichment at H4 might be of primary nature, caused by localized B-rich source material.

Boron isopleths from traverse A (Fig. 4a) indicate possible strata-bound B enrichment for a distance of at least 67 m between boreholes H2 and H3. The two apparent B-rich layers dip towards the west edge of the dam, consistent with the gradient of the 2004 groundwater table, and taper down to background levels towards H1 on the edge of the dam (Fig. 4a). Downward infiltration in the clay-rich layers immediately below the coarse layers allowed B to be absorbed and enriched by the less permeable material, whereas B discharge occurred in layers of higher permeability. By construction, the margin of the tailings dam consists of sand-rich, coarse-grained sediment, pushed up repeatedly to confine the tailings (Lottermoser 2010 and references therein). Assuming a secondary B redistribution, this coarser material may have facilitated the flow of B towards the edge of the dam, following the path of highest permeability, allowing the soluble B to be washed out near borehole H1. Consequently, the low B levels in H1 can be attributed to the general lack of silt to clay-sized tailings sediment and the westward discharge of B (Figs. 3, 4a, 6).

Data in the northern traverse B (Fig. 4b) indicate that B is most concentrated near the edge of the tailings dam, represented by two B-rich plumes in H4 and another plume near the bottom of H6. According to the borehole observations, we encountered water-saturated tailings underlain by a thin soil and natural coarse sand and gravel in traverse B (with no impermeable liner) at elevations between 317 and 313 m (Fig. 4b; Appendix 1). These observations were consistent with the 2004 water table reported by AMEC (2005), although the 2010 water table level appeared to be higher by 1–2 m. Traverse B data suggest that B discharges below the tailings catchment, or along a possible layer of high permeability at ≈315 m. Although a detailed grain-size analysis of this traverse is necessary to better constrain the effects of subsurface permeability, it seems likely that gravels underlying the tailings in this area provide another path of B discharge and transport out of Dam No. 5.

Finally, near-surface samples in most of the boreholes are characterized by low B concentrations that appear to correlate with tan-beige colored sediment. These surface layers are typically underlain by dark gray or bluish-grey, unoxidized sediment. This color transition is most likely due to meteoric water seepage causing iron oxidation.

mine, and thus an important constituent of the tailings. The high abundance of Mg and B in the tailings is also consistent with the occurrence of the efflorescent hydrous Mg-borate, along a continuous layer ≈100 m long and ≈1–2 m thick on the western edge of Dam No. 5 (Fig. 2).

Fig. 6 Grain-size analysis and boron leachability for tailings along Traverse A: Left: Fraction of grains ≤38 μm (wt%) versus leached B (mg/L). Legend shows depth (m) of sampled intervals. *Right*: grain-size distribution histograms of selected samples in cumulative wt%. Legend shows depth (m) of representative samples from each interval shown on the *left*
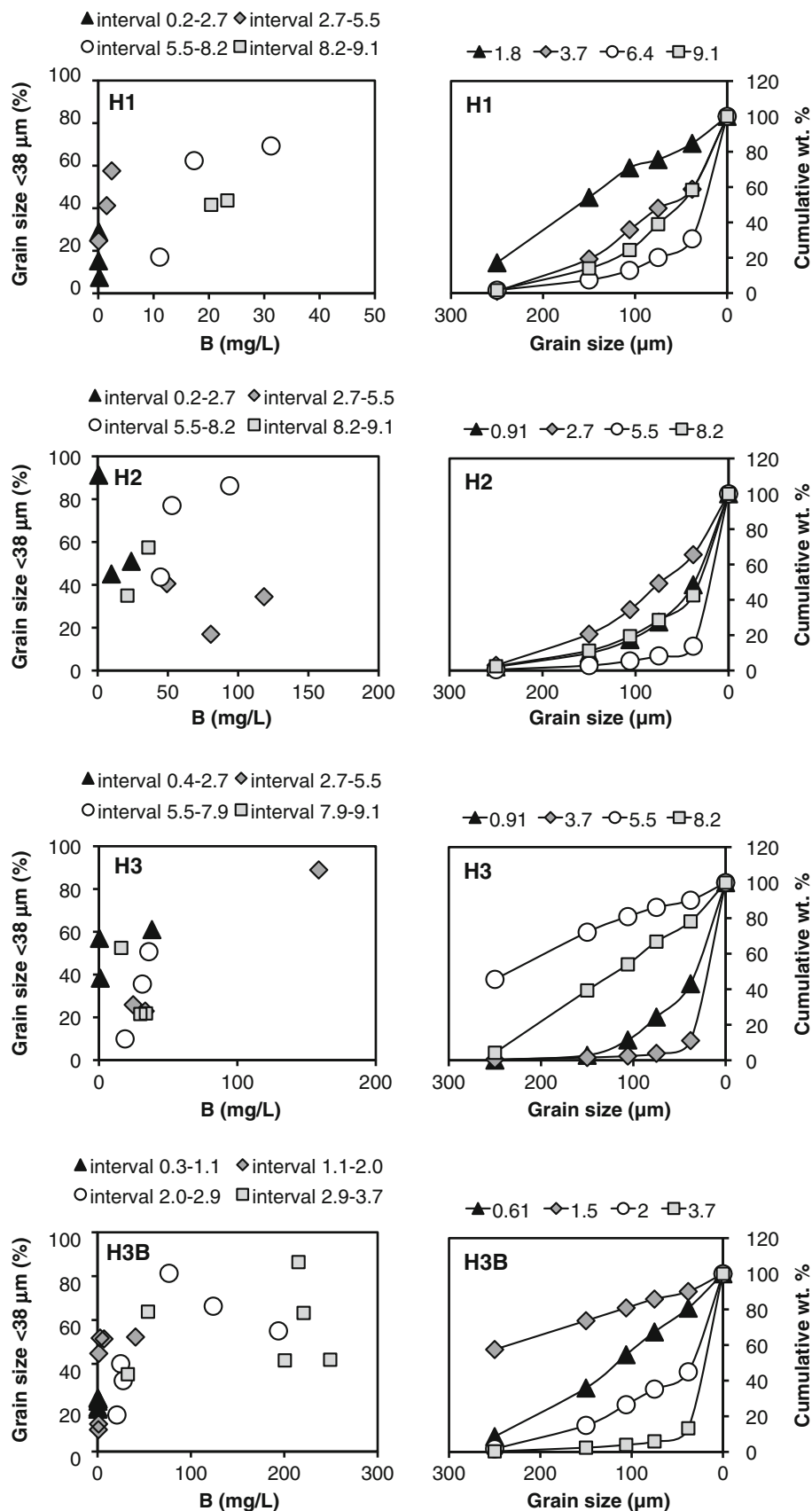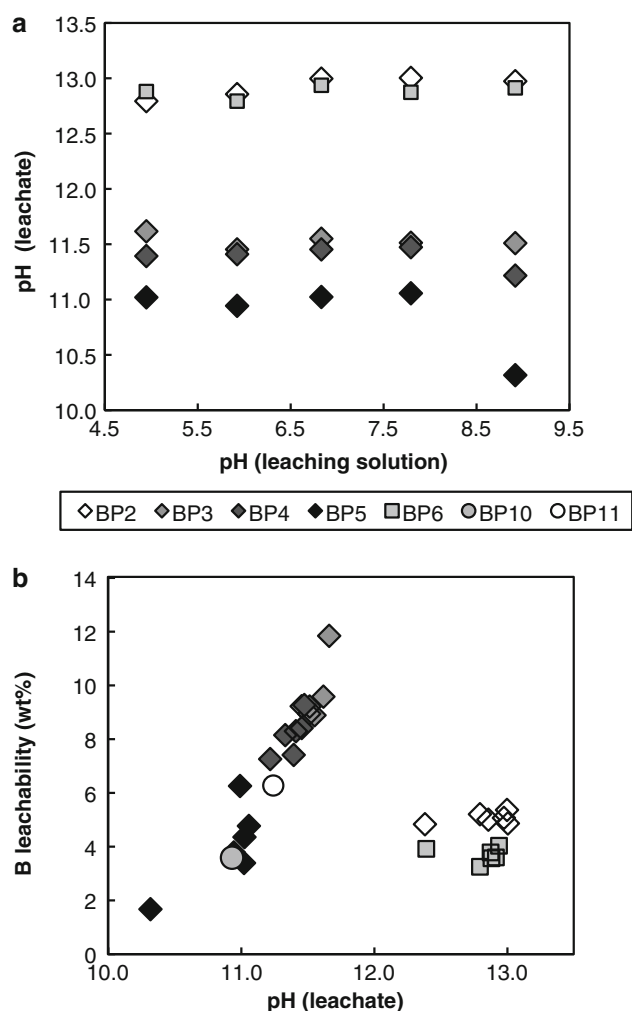
Fig. 7 Boron leachability in leaching solutions of variable pH for seven slag samples: **a** final pH of the leachate solutions after 24 h leaching versus initial pH of the leaching solutions; **b** B leachability (wt% of initial solid slag) versus the final pH of the leachate solution (see text for more explanations). *Diamonds* Dome; *squares* Bell Creek; *circles* Lake Shore; *solid symbols* refinery slags; *open symbols* assay lab slags. For sample abbreviation and description see Table 1

Meteoric water infiltration also resulted in depletion of B in the surface layer and remobilization of B, leading to localized B enrichment in the grey colored, clay-rich sediment and the eventual discharge of B into the surrounding environment.

Possible Sources of Boron

We propose two end-member sources for the initial B-enrichments in McIntyre Tailings Dam No. 5: (1) primary B of natural origin deposited in the tailings slurry and; (2) B introduced as borax flux in the assaying and refining the gold ore, deposited as waste in Dam No. 5, and subsequently remobilized by groundwater and meteoric

water flow. In such a stratigraphically complex, open system, a mixture of the two end-member sources could be responsible for the observed B distribution.

As noted above, potential natural sources of B include: weathering of tourmaline, B-rich fluid inclusions, carbonates or anhydrite containing B, or carbonate-altered B-rich tholeiitic basalts. The stability of tourmaline over a broad pH range and its resistance to weathering make tourmaline dissolution an unlikely major source of soluble B (Graham 1957). B concentrations in fluid inclusions from quartz veins from the Hollinger and McIntyre Mines are highly variable, but generally low (Sirbescu, unpubl.). The B released from fluid inclusions during and after tailings processing would be too low to account for the high concentrations measured in Dam No. 5 (Paliewicz et al. 2012). Furthermore, LA–ICP–MS analyses of anhydrite found that the average value of 4.6 mg/kg of detected B was also much too small to be a major contributor of the B found in the tailings.

Boron-rich tholeiitic basalts affected by carbonate alteration are a more plausible source of primary B in the McIntyre tailings. However, it is important to note that anomalous B was only detected at McIntyre Tailings Dam No. 5 and in no other tailings dam sites in the Timmins area (AMEC 2005; Sulatycky, personal commun.). The altered tholeiitic basalts are common to the entire Porcupine-Timmins gold camp and there is no reason why they would be preferentially deposited in Dam No. 5. Therefore, the B anomaly is most likely derived from the $\approx$60,000 t of imported borax-fluxed slag and refinery bricks processed between 1985 and 1991 by the GoMill custom milling circuit (Pamour Porcupine Mine Manager Monthly Reports 1984–1991; Yeoman, written communiqué). Indeed, our 24 h tests of slag leachability in distilled water and variable pH solutions confirm that pulverized slag from two current Timmins gold mine refineries and their fire assaying labs release at least an order of magnitude more B than all the B contained in the carbonate-altered basaltic rocks. Therefore, it is highly probable that the crushed slag waste from GoMill, after interaction with meteoric or tailings water, accounts for most of the soluble B anomalies observed in Tailings Dam No. 5. The localized, semi-continuous layered distribution of B anomalies within <9 m of tailings investigated in this study is consistent with the spigotting method of slurry discharge within the impoundment dam. Although the period of slag disposal started in 1984, 3 years after the central-northern section of Dam No. 5 started to being filled with regular processed-ore waste, our data from section B show that the B anomalies infiltrated downwards. This remobilization explains the presence of B contamination in tailings deposited before 1984.

The rapid release of B from slags from precious metal refinery processes discarded directly onto tailings should be a matter of concern for existing and future operations. Other contaminants, such as As, Mo, Pb, and Hg, may also contaminate ground or surface waters if they preferentially partition into the alkaline, B-rich solutions. In addition, the future use of B as a flux in metallurgical extraction is likely going to increase. The use of borax has been proposed as an alternative to Hg amalgamation for gold extraction in small-scale operations in underdeveloped countries, since borax has far milder health consequences than mercury (Appel and Na-Oy 2012), without properly assessing the magnitude of B contamination relative to world drinking water guidelines.

Conclusions

The distribution of anomalous concentrations of leachable B in Tailings Dam No. 5, as indicated by tailings leachate chemistry and grain-size analysis, indicates that B is typically adsorbed and concentrated at or above layers containing mostly silt–clay grains (≤ 38 μm). Discharge of B along the western edge of Dam No. 5 contributed to the redistribution of B anomalies and resulted in the precipitation of Mg-borates along the edge of the dam. The distribution of B-contaminated areas is ephemeral and most likely fluctuates with meteoric precipitation and changes in the local water table. The B absorbed onto fine-grained material appears to have a much longer residence time, explaining why B anomalies are still present after more than 20 years.

Our preliminary slag-leachability tests support our hypothesis that borax used in gold refining is the main source of the B anomalies at Dam No. 5. The amount of B leached from the tested slag exceeds the B potentially released from primary natural sources by orders of magnitude. Tourmaline, anhydrite, or fluid inclusions in the tailings are negligible sources of B. B-rich carbonate-altered tholeiitic basalts might explain (at least in part) the elevated concentrations of B. However, if the widespread host-rock were a major source of B, similar B anomalies would be expected in the other four McIntyre dams that

were active simultaneously with Dam No. 5. A future, broader study on B isotopes and B leachability of tailings, slags, refinery bricks, and of host rocks is needed to unambiguously constrain the anthropogenic versus natural sources of B in the tailings.

It is important to note that the amount of B leachable from McIntyre tailings was detected at toxic and even lethal concentrations. Based on the available data, the distribution of B contamination in gold mine tailings is complex, uneven, and ephemeral; therefore, the discharge of B into the surroundings is difficult to assess. B contamination from mine wastes and the resulting environmental harm could easily go unnoticed at other tailings with similar pyrometallurgical practices. Currently, B-fluxed slag from gold refineries and lab assaying is being reintroduced into some of the mill concentration circuits in the Porcupine–Timmins gold camp, so that soluble B is largely diluted before being discarded on tailings. However, remediation studies of older tailings such as McIntyre should determine whether substantial slag was disposed of without recycling and assess the magnitude, distribution, and sources of B contamination.

Supplementary data associated with this article can be found in "Appendixes 1 and 2" in the online version of this paper, which can be downloaded for free by all subscribers.

Appendix 1

See Table 2.

Table 2 Boron concentration in tailings leachates and ground water samples from McIntyre Dam 5
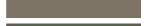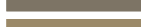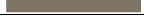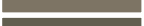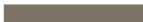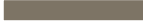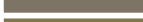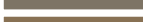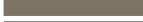
Sample	Depth	Elev.	Boron (mg/L)	Fraction <38μm (wt%)	Munsell Color (Wetted)	
Borehole H1						
H1-1	0.2	325.0	0.2	7.5	2.5y 4/2 dark grayish brown	
H1-2	0.9	324.3	0.1	28.8	2.5y 4/3 olive brown	
H1-3	1.8	323.4	0.0	15.3	5y 4/2 olive gray	
H1-4	2.7	322.5	0.1	24.7	5y 4/3 olive	
H1-5	3.7	321.6	1.5	41.2	5y 4/2 olive gray	
H1-6	4.6	320.7	2.4	57.6	5y 3/2 dark olive gray	
H1-7	5.5	319.8	17.3	62.4	5y 3/2 dark olive gray	
H1-8	6.4	318.8	31.2	69.3	5y 4/2 olive gray	
H1-9	7.3	317.9	11.1	17.0	5y 4/2 olive gray	
H1-10	8.2	317.0	23.3	43.7	5y 4/3 olive	
H1-11	9.1	316.1	20.4	41.6	5y 3/2 dark olive gray	
Borehole H2						
H2-1	0.2	323.0	0.8	91.2	2.5y 5/4 light olive brown	
H2-2	0.9	322.3	23.9	51.0	5y 5/2 olive gray	
H2-3	1.8	321.4	9.8	45.1	2.5y 5/4 light olive brown	
H2-4	2.7	320.5	118.4	34.5	5y 4/1 dark gray	
H2-5	3.7	319.6	49.3	40.5	5y 4/2 olive gray	
H2-6	4.6	318.7	80.5	16.9	5y 3/1 very dark gray	
H2-7	5.5	317.8	94.0	86.2	5y 4/2 olive gray	
H2-8	6.4	316.8	52.9	77.0	5y 4/2 olive gray	
H2-9	7.3	315.9	44.7	43.6	5y 4/2 olive gray	
H2-10	8.2	315.0	36.1	57.4	5y 5/3 olive	
H2-11	9.1	314.1	21.2	35.0	5y 4/2 olive gray	
Borehole H3						
H3-1	0.4	322.6	1.0	38.3	2.5y 5/4 light olive brown	
H3-2	0.9	322.1	0.4	56.9	5y 5/3 olive	
H3-3	1.8	321.2	38.3	61.0	5y 5/2 olive gray	
H3-4	2.7	320.3	24.7	25.9	5y 5/2 olive gray	
H3-5	3.7	319.3	158.8	88.9	5y 5/1 gray	
H3-6	4.6	318.4	33.5	22.9	gley2 4/5pb dark bluish gray	
H3-7	5.5	317.5	18.9	9.9	5y 4/2 olive gray	
H3-8	6.4	316.6	31.4	35.6	5y 4/1 dark gray	
H3-9	7.3	315.7	36.0	50.7	5y 4/1 dark gray	
H3-10	7.9	315.1	29.9	21.6	5y 4/1 dark gray	
H3-11	8.2	314.8	34.0	21.8	5y 4/1 dark gray	
H3-12	9.1	313.9	16.1	52.5	5y 4/2 olive gray	
Borehole H3B						
H3B-1	0.3	322.7	0.4	20.2	2.5y 4/3 olive brown	
H3b-2	0.5	322.5	0.3	24.5	2.5y 4/4 olive brown	
H3b-3	0.6	322.4	0.3	19.3	5y 4/3 olive	
H3b-4	0.8	322.2	0.5	23.0	5y 4/3 olive	
H3B-5	0.9	322.1	0.8	24.0	5y 4/3 olive	
H3b-6	1.1	321.9	1.3	44.7	2.5y 5/4 light olive brown	
H3b-7	1.2	321.8	2.8	51.8	5y 5/2 olive gray	
H3b-8	1.4	321.6	1.1	12.6	2.5y 4/4 olive brown	
H3b-9	1.5	321.5	0.9	10.0	5y 4/4 olive	
H3b-10	1.7	321.3	7.0	51.4	5y 5/2 olive gray	
H3B-11	1.8	321.2	40.7	52.2	5y 4/2 olive gray	
H3b-12	2.0	321.0	193.7	55.0	5y 4/2 olive gray	
H3B-13	2.1	320.9	123.9	66.3	5y 5/1 gray	
H3B-14	2.3	320.7	76.6	81.3	5y 5/2 olive gray	
H3B-15	2.4	320.6	27.5	32.4	5y 5/2 olive gray	
H3B-16	2.6	320.4	24.8	40.1	5y 5/2 olive gray	
H3B-17	2.7	320.3	20.8	16.7	5y 4/1 dark gray	
H3B-18	2.9	320.1	32.4	35.3	5y 4/2 olive gray	
H3B-19	3.0	320.0	54.0	63.8	5y 5/2 olive gray	
H3B-20	3.2	319.8	249.2	41.9	5y 5/1 gray	
H3B-21	3.4	319.6	200.6	41.6	5y 4/1 dark gray	
H3B-22	3.5	319.5	220.7	63.2	5y 4/1 dark gray	
H3B-23	3.7	319.3	215.2	86.4	5y 5/1 gray	

Table 2 continued

Sample	Depth	Elev.	Boron (mg/L)	Fraction <38μm (wt%)	Munsell Color (wetted)	
					Borehole H4	
H4-1	0.2	322.8	13.0		2.5y 4/4 olive brown	
H4-2	0.9	322.1	25.2		5y 4/2 olive gray	
H4-3	1.8	321.2	139.3		5y 4/1 dark gray	
H4-4	2.7	320.3	42.0		5y 4/2 olive gray	
H4-5	3.7	319.3	29.8		5y 2.5/1 black	
H4-6	4.6	318.4	54.9		5y 4/3 olive	
H4-7	5.5	317.5	91.3		5y 4/2 olive gray	
H4-8	6.4	316.6	134.2		2.5y 4/2 dark grayish brown	
H4-9	7.3	315.7	58.0	tailings	5y 4/3 olive	
H4-9b	7.5	315.5	56.3	glacial sed.	5y 4/2 olive gray	
H4-9c	7.6	315.4	44.0		10yr 4/4 dark yellowish brown	
H4-10	8.2	314.8	15.3		2.5y 5/3 light olive brown	
					Borehole H5	
H5-1	0.2	321.8	3.0		10yr 5/6 yellowish brown	
H5-2	0.9	321.1	2.6		10yr 4/6 dark yellowish brown	
H5-3	1.8	320.2	41.8		5y 5/2 olive gray	
H5-4	2.7	319.3	8.4		5y 4/2 olive gray	
H5-5	3.7	318.3	15.8		5y 3/1 very dark gray	
H5-6	4.6	317.4	33.0		5y 3/2 dark olive gray	
H5-7	5.5	316.5	24.6		5y 4/2 olive gray	
H5-8	6.4	315.6	35.2		5y 4/3 olive	
H5-9	7.3	314.7	37.7	tailings	5y 4/3 olive	
H5-10	7.7	314.3	40.9	glacial sed.	5y 4/2 olive gray	
H5-11	7.8	314.2	52.7		10yr 3/3 dark brown	

Hole H3		**3-1(a)**	**3-1(b)**	**3-2**	**3-3**	**3-4**	**3-5**	**3-6**	**3-7**	**3-8**	**3-9**	**3-10**	**3-11**	**3-12**

Sample	Depth	Elev.	Boron (mg/L)	Fraction <38μm (wt%)	Munsell Color (wetted)	
					Borehole H6	
H6-1	0.2	321.3	8.5		5y 4/2 olive gray	
H6-2	0.9	320.6	13.5		2.5y 5/4 light olive brown	
H6-3	1.8	319.7	70.1		5y 4/3 olive	
H6-4	2.7	318.8	48.1		5y 4/3 olive	
H6-5	3.7	317.8	66.5		5y 4/3 olive	
H6-6	4.6	316.9	82.8		5y 4/3 olive	
H6-7	5.5	316.0	82.7		5y 4/3 olive	
H6-8	6.4	315.1	88.5		5y 3/2 dark olive gray	
H6-9	7.3	314.2	16.5	tailings	5y 4/1 dark gray	
H6-9B	7.9	313.6	20.4	glacial sed.	5y 3/2 dark olive gray	
H6-10	8.2	313.3	21.5		2.5y 3/3 dark olive brown	
H6-11	8.8	312.7	10.3		2.5y 4/4 olive brown	
					Borehole H7	
H7-1	0.3	324.7	0.0		10yr 3/6 dark yellowish brown	
H7-2	0.9	324.1	0.0		2.5y 5/6 light olive brown	
H7-3	1.5	323.5	7.1		2.5y 4/4 olive brown	
H7-4	1.7	323.3	0.0		2.5y 4/4 olive brown	
H7-5	1.8	323.2	0.0		2.5y 4/4 olive brown	
H7-6	2.0	323.0	0.3		5y 4/4 olive	
H7-7	2.1	322.9	0.0		5y 4/4 olive	
H7-8	2.3	322.7	0.0		5y 4/4 olive	
H7-9	2.4	322.6	0.0		5y 4/4 olive	
H7-10	2.6	322.4	0.0		5y 4/2 olive gray	
H7-11	2.7	322.3	0.0		5y 5/2 olive gray	
H7-12	2.9	322.1	0.0		5y 5/3 olive	
H7-13	3.0	322.0	0.6		5y 4/3 olive	
H7-14	3.2	321.8	0.2		5y 4/3 olive	
H7-15	3.4	321.6	0.2		5y 4/3 olive	
H7-16	3.5	321.5	0.2		5y 4/3 olive	
H7-17	3.7	321.3	0.2		5y 5/3 olive	
H7-18	3.8	321.2	0.2		5y 4/4 olive	
H7-19	4.0	321.0	0.2		5y 5/3 olive	
H7-20	4.1	320.9	0.3		5y 5/3 olive	
H7-21	4.3	320.7	0.2		5y 5/3 olive	

Table 2 continued

Sample	Depth	Elev.	Boron (mg/L)	Fraction <38μm (wt%)				Munsell Color (Wetted)					Sample		
Hole H3		3-1(a)	3-1(b)	3-2	3-3	3-4	3-5	3-6	3-7	3-8	3-9	3-10	3-11	3-12
				Borehole H7											
H7-22	4.4	320.6	3.6				5y 4/2 olive gray								
H7-23	4.6	320.4	7.7				5y 3/2 dark olive gray								
H7-24	4.7	320.3	18.7				5y 4/2 olive gray								
H7-25	4.9	320.1	16.1				5y 3/2 dark olive gray								
H7-26	5.0	320.0	22.3				5y 4/2 olive gray								
H7-27	5.2	319.8	18.9				5y 4/2 olive gray								
H7-28	5.3	319.7	8.4				5y 2.5/1 black								
H7-29	5.5	319.5	4.4				5y 2.5/1 black								
H7-30	5.6	319.4	4.9				5y 3/1 very dark gray								
Ground water samples															
Sample	**Boron (mg/L)**														
GW-W1	81.3														
GW-W2	20.2														

The silt + clay fraction (grain size <38 μm) is shown in mass %. The Munsell color of each homogenized sample in a wetted state is reported using standard hue color/chroma notation, followed by Munsell color name. The water table is shown with a *blue dashed line*. The bottom of tailings is indicated with a *double solid line*. Depth and elevation above sea level and below the surface are in meters, based on the bottom of the tailings

Appendix 2

See Table 3.

Table 3 Timmins mine tailings–wet sieve data sheet

Hole H3	3-1(a)	3-1(b)	3-2	3-3	3-4	3-5	3-6	3-7	3-8	3-9	3-10	3-11	3-12
Grain size (μm)	*Grain size distribution (%)*												
>250 (concretions)	0.0	0.0	0.0	0.0	0.0	0.0	0.0	0.0	0.0	0.0	0.0	0.0	0.0
250	7.6	0.0	0.1	3.8	14.0	0.5	3.6	45.5	2.1	2.4	12.3	4.2	0.7
150	15.3	17.4	2.7	4.6	26.2	1.0	25.0	26.6	15.3	11.4	35.2	35.1	6.8
106	16.5	18.1	8.6	5.3	10.4	0.8	23.8	8.8	13.6	8.9	11.0	14.7	11.6
75	16.1	13.1	12.9	6.5	12.5	1.5	15.3	5.2	14.6	9.1	10.5	12.8	11.0
38	13.5	13.1	18.8	18.8	10.9	7.2	9.5	4.0	18.7	17.5	9.4	11.4	17.4
<38	30.9	38.3	56.9	61.0	25.9	88.9	22.9	9.9	35.6	50.7	21.6	21.8	52.5
	100	100	100	100	100	100	100	100	100	100	100	100	100
Grain size (μm)	*Total cumulative (%)*												
>250 (concretions)	0.0	0.0	0.0	0.0	0.0	0.0	0.0	0.0	0.0	0.0	0.0	0.0	0.0
250	7.6	0.0	0.1	3.8	14.0	0.5	3.6	45.5	2.1	2.4	12.3	4.2	0.7
150	23.0	17.4	2.8	8.3	40.3	1.6	28.6	72.1	17.4	13.8	47.5	39.3	7.6
106	39.4	35.5	11.4	13.6	50.7	2.4	52.4	80.9	31.1	22.7	58.5	54.0	19.2
75	55.5	48.6	24.3	20.1	63.2	3.9	67.6	86.1	45.7	31.8	69.0	66.8	30.2
38	69.1	61.7	43.1	39.0	74.1	11.1	77.1	90.1	64.4	49.3	78.4	78.2	47.5
<38	100	100	100	100	100	100	100	100	100	100	100	100	100
Boron (ppm)	1.0	1.0	0.4	38.3	24.7	158.8	33.5	18.9	31.4	36.0	29.9	34.0	16.1
Depth (m)	0.00	0.4	0.9	1.8	2.7	3.7	4.6	5.5	6.4	7.3	7.9	8.2	9.1

Hole H3B	3B-1	3B-2	3B-3	3B-4	3B-5	3B-6	3B-7	3B-8	3B-9	3B-10	3B-11	3B-12	3B-13
Grain size (μm)	*Grain size distribution (%)*												
>250 (concretions)	0.0	0.0	0.0	0.0	0.0	0.0	0.0	0.0	0.0	0.0	0.0	0.0	0.0
250	6.3	4.9	8.6	16.8	2.3	1.6	0.6	27.6	57.5	10.4	3.3	1.7	2.2
150	27.4	26.0	27.3	27.9	23.0	15.0	11.0	29.3	16.2	12.6	14.3	13.2	2.3
106	17.9	12.7	18.7	10.2	19.1	11.1	12.4	10.4	7.2	9.4	9.1	11.6	3.2
75	16.1	18.9	12.8	12.4	15.4	12.7	10.8	11.9	4.9	6.8	7.6	8.8	8.2
38	12.1	13.0	13.4	9.7	16.2	14.8	13.4	8.2	4.3	9.5	13.6	9.7	17.8

Table 3 continued

Hole H3B	3B-1	3B-2	3B-3	3B-4	3B-5	3B-6	3B-7	3B-8	3B-9	3B-10	3B-11	3B-12	3B-13
<38	20.2	24.5	19.3	23.0	24.0	44.7	51.8	12.6	10.0	51.4	52.2	55.0	66.3
	100	100	100	100	100	100	100	100	100	100	100	100	100

Hole H3B	3B-1	3B-2	3B-3	3B-4	3B-5	3B-6	3B-7	3B-8	3B-9	3B-10	3B-11	3B-12	3B-13
Grain size (µm)	Total cumulative (%)												
>250 (concretions)	0	0	0	0	0	0	0.0	0.0	0.0	0.0	0.0	0.0	0.0
250	6.3	4.9	8.6	16.8	2.3	1.6	0.6	27.6	57.5	10.4	3.3	1.7	2.2
150	33.7	31.0	35.9	44.7	25.3	16.6	11.7	56.9	73.6	23.0	17.5	14.9	4.6
106	51.6	43.7	54.6	54.9	44.4	27.7	24.1	67.3	80.8	32.3	26.6	26.5	7.7
75	67.7	62.6	67.3	67.3	59.8	40.4	34.8	79.3	85.8	39.1	34.2	35.2	15.9
38	79.8	75.5	80.7	77.0	76.0	55.3	48.2	87.4	90.0	48.6	47.8	45.0	33.7
<38	100	100	100	100	100	100	100	100	100	100	100	100	100
Boron (ppm)	0.4	0.3	0.3	0.5	0.8	1.3	2.8	1.1	0.9	7.0	40.7	193.7	123.9
Depth (m)	0.3	0.5	0.6	0.8	0.9	1.1	1.2	1.4	1.5	1.7	1.8	2.0	2.1

Hole H3B cont'd	3B-14	3B-15	3B-16	3B-17	3B-18	3B-19	3B-20	3B-21	3B-22	3B-23
Grain size (µm)	Grain size distribution (%)									
>250 (concretions)	2.1	0.0	0.0	0.0	0.0	0.0	1.2	1.3	0.0	0.3
250	0.3	1.6	2.6	18.1	9.0	2.2	0.8	1.4	0.2	0.3
150	1.1	20.8	13.2	35.5	24.3	4.8	6.6	11.7	4.2	2.1
106	1.1	21.7	16.1	13.2	12.1	4.9	12.0	11.3	5.7	1.6
75	2.8	11.7	13.9	9.1	8.5	7.6	14.5	14.9	10.0	1.9
38	11.3	11.8	14.2	7.3	10.8	16.6	23.1	17.8	16.7	7.3
<38	81.3	32.4	40.1	16.7	35.3	63.8	41.9	41.6	63.2	86.4
	100	100	100	100	100	100	100	100	100	100
Grain size (µm)	Total cumulative (%)									
>250 (concretions)	2.1	0.0	0.0	0.0	0.0	0.0	1.2	1.3	0.0	0.3
250	2.4	1.6	2.6	18.1	9.0	2.2	2.0	2.7	0.2	0.6
150	3.6	22.4	15.8	53.7	33.4	7.1	8.6	14.5	4.4	2.7
106	4.6	44.1	31.9	66.9	45.4	11.9	20.6	25.7	10.1	4.3
75	7.4	55.9	45.8	76.0	53.9	19.6	35.0	40.6	20.1	6.2
38	18.7	67.6	59.9	83.3	64.7	36.2	58.1	58.4	36.8	13.6
<38	100	100	100	100	100	100	100	100	100	100
Boron (ppm)	76.6	27.5	24.8	20.8	32.4	54.0	249.2	200.6	220.7	215.2
Depth (m)	2.3	2.4	2.6	2.7	2.9	3.1	3.2	3.4	3.5	3.7

Hole H2	H2-1	H2-2	H2-3	H2-4	H2-5	H2-6	H2-7	H2-8	H2-9	H2-10	H2-11
Grain size (µm)	Grain size distribution (%)										
>250 (concretions)	0.0	0.5	1.6	0.0	0.0	0.0	0.0	0.0	0.0	0.0	0.0
250	0.1	1.6	2.5	2.9	2.9	4.9	0.5	0.8	5.7	2.4	1.9
150	0.6	8.2	17.9	17.7	20.3	30.8	2.3	4.0	19.1	8.8	17.3
106	1.2	7.7	12.3	13.8	12.4	8.5	2.6	4.5	11.3	8.2	20.0
75	2.0	10.0	10.8	14.8	10.7	27.0	2.9	5.0	9.3	9.2	12.9
38	5.0	21.1	9.8	16.3	13.2	11.8	5.5	8.6	10.9	14.0	12.9
<38	91.2	51.0	45.1	34.5	40.5	16.9	86.2	77.0	43.6	57.4	35.0
	100	100	100	100	100	100	100	100	100	100	100
Grain size (µm)	Total cumulative (%)										
>250 (concretions)	0.0	0.5	1.6	0.0	0.0	0.0	0.0	0.0	0.0	0.0	0.0

Table 3 continued

Hole H2	H2-1	H2-2	H2-3	H2-4	H2-5	H2-6	H2-7	H2-8	H2-9	H2-10	H2-11
250	0.1	2.1	4.1	2.9	2.9	4.9	0.5	0.8	5.7	2.4	1.9
150	0.6	10.3	22.0	20.6	23.2	35.8	2.8	4.8	24.9	11.2	19.2
106	1.8	17.9	34.3	34.4	35.6	44.3	5.4	9.3	36.1	19.4	39.2
75	3.7	27.9	45.1	49.3	46.3	71.3	8.3	14.4	45.5	28.6	52.1
38	8.8	49.0	54.9	65.5	59.5	83.1	13.8	23.0	56.4	42.6	65.0
<38	100	100	100	100	100	100	100	100	100	100	100
Boron (ppm)	0.7	23.9	9.8	118.4	49.3	80.5	93.9	52.9	44.7	36.1	21.2
Depth (m)	0.2	0.9	1.8	2.7	3.7	4.6	5.5	6.4	7.3	8.2	9.2

Hole H1	H1-1	H1-2	H1-3	H1-4	H1-5	H1-6	H1-7	H1-8	H1-9	H1-10	H1-11
Grain size (μm)	*Grain size distribution (%)*										
>250 (concretions)	0.0	0.0	0.0	0.0	0.0	0.0	0.0	0.0	0.0	0.0	0.0
250	29.8	4.3	17.2	4.4	1.0	0.3	0.5	1.6	7.7	3.4	1.6
150	39.7	17.8	37.0	23.6	18.3	2.4	4.0	5.8	34.6	16.0	12.4
106	14.1	16.9	16.7	20.9	16.5	5.9	4.5	5.4	25.4	11.3	10.4
75	5.6	15.0	4.7	14.2	12.2	11.6	8.1	7.3	7.3	10.2	14.6
38	3.4	17.1	9.2	12.3	10.7	22.2	20.5	10.5	8.0	15.5	19.4
<38	7.5	28.8	15.3	24.7	41.2	57.6	62.4	69.3	17.0	43.7	41.6
	100	100	100	100	100	100	100	100	100	100	100
Grain size (μm)	*Total cumulative (%)*										
>250 (concretions)	0.0	0.0	0.0	0.0	0.0	0.0	0.0	0.0	0.0	0.0	0.0
250	29.8	4.3	17.2	4.4	1.0	0.3	0.5	1.6	7.7	3.4	1.6
150	69.5	22.1	54.1	28.0	19.3	2.7	4.5	7.5	42.2	19.4	14.0
106	83.5	39.0	70.9	48.8	35.9	8.7	9.0	12.8	67.7	30.7	24.4
75	89.2	54.1	75.5	63.1	48.0	20.3	17.1	20.2	74.9	40.9	39.0
38	92.5	71.2	84.7	75.3	58.8	42.4	37.6	30.7	83.0	56.3	58.4
<38	100	100	100	100	100	100	100	100	100	100	100
Boron (ppm)	0.2	0.1	0.0	0.1	1.5	2.4	17.3	31.2	11.1	23.3	20.4
Depth (m)	0.2	0.9	1.8	2.7	3.7	4.6	5.5	6.4	7.3	8.2	9.2

References

AMEC (2005) Geotechnical and environmental tailings closure assessment McIntyre tailings dam. AMEC America's Limited Earth & Environmental Div, Lively, Ontario

Annovitz LM, Grew ES (1996) Mineralogy, petrology, and geochemistry of boron: an introduction. In: Grew, ES, Anovitz, LM (eds) Boron mineralogy, petrology, and geochemistry. Rev Mineral 33:1–30

Appel PWU, Na-Oy L (2012) The borax method of gold extraction for small-scale miners. J Health Pollution 2:5–10

Bateman R, Ayer JA, Dubé B Hamilton MA (2005) The Timmins–Porcupine gold camp, Northern Ontario: the anatomy of an archaean greenstone belt and its gold mineralization: discover Abitibi Initiative. Ontario Geological Survey Open File Rept 6158, accessible at: http://www.geologyontario.mndmf.gov.on.ca/mndmfiles/pub/data/imaging/OFR6158/OFR6158.pdf

Black JA, Barnum JB, Birge WJ (1993) An integrated assessment of the biological effects of boron to the rainbow trout. Chemosphere 26:1383–1413

Bugbee EE (1981) A textbook of fire assaying. Willey, New York City

Cano-Reséndiz O, de la Rosa G, Cruz-Jiménez G, Gardea-Torresdey JL, Robinson BH (2011) Evaluating the role of vegetation on the transport of contaminants associated with a mine tailing using the Phyto-DSS. J Hazard Mater 189:472–478

Dionisiou NMT, Misopolinos ND (2006) Surface water quality—use of magnesia for boron removal from irrigation water. J Environ Qual 35:2222–2228

Dydo P, Turek M (2013) Boron transport and removal using ion-exchange membranes: a critical review. Desalination 310:2–8

Figen AK, Pişkin S (2010) Parametric investigation of anhydrous sodium metaborate ($NaBO_2$) synthesis from concentrated tincal. Adv Powder Technol 21:513–520

Fyon JA, Crocket JH (1982) Gold exploration in the timmins district using field and lithogeochemical characteristics of carbonate alteration zones. Can Inst Min Metall Geol Can Gold Depos Spec 24:113–129

Gemici Ü, Tarcan C, Helvaci C, Somay AM (2008) High arsenic and boron concentrations in groundwaters related to mining activity in the Bigadiç borate deposits (Western Turkey). Appl Geochem 23:2462–2476

Goldberg S, Suarez DL (2011) Influence of soil solution cation composition on boron adsorption by soils. Soil Sci 126:80–83

Graham ER (1957) The weathering of some boron-bearing materials. Soil Sci Soc Am 21:505–508

Guilbert JM, Park CF (2007) The geology of ore deposits. Waveland Press, Long Grove

Hayashi S, Takahasi T, Kanehashi K, Kubota N, Kashiwakura S, Sakamoto T, Nagasaka T (2010) Chemical state of boron in coal fly ash investigated by focused-ion-beam time-of-flight secondary ion mass spectrometry (FIB-TOF-SIMS) and satellite-transition magic angle spinning nuclear magnetic resonance (STMAS NMR). Chemosphere 80:881–887

Health Canada (2012) Guidelines for Canadian drinking water quality—Summary Table. Water, air and climate change Bureau, healthy environments and consumer safety branch, Health Canada, Ottawa, ON; accessed 03 Jan 2014 at http://www.hc-sc.gc.ca/ewh-semt/pubs/water-eau/2012-sum_guide-res_recom/index-eng.php

Hudson-Edwards KA, Jamieson HE, Lottermoser BG (2011) Mine wastes: past, present, future. Elements 7:375–380

Iwashita A, Sakaguchi Y, Nakajima T, Takanashi H, Ohki A, Kambara S (2005) Leaching characteristics of boron and selenium for various coal fly ashes. Fuel 84:479–485

Jamieson HE (2011) Geochemistry and mineralogy of solid mine waste: essential knowledge for predicting environmental impact. Elements 7:381–386

Kent PA (1988) Dec 15, 1988 Memo from Noranda Sales Corp to Mr. Peter Rowlandson about contract renewal, GoldCorp Archives, Timmins, ON, Canada

Leeman WP, Sisson VB (1996) Geochemistry of boron and its implications for crustal and mantle processes. In: Grew, ES, Anovitz, LM (eds) Boron mineralogy, petrology, and geochemistry, Rev Mineral 33:645–695

Lottermoser BG (2010) Mine Wastes: characterization, treatment, environmental impacts, 3rd edn. Springer-Verlag, Berlin

Marsden J, House I (2006) The Chemistry of Gold Extraction. 2nd Edit, Soc for Mining, Metallurgy, and Exploration (SME), Littleton, CO, USA

McDonough WF, Sun S-S (1995) The composition of the Earth. Chem Geol 120:223–253

Mine Manager Monthly Reports (1984) Monthly reports written by various mine managers to the corporate head office that detail the development and production activity of the various Pamour Porcupine mines and mills. GoldCorp Archives, Timmins

Munsell® Color Charts (2010) Year 2000 Revised Washable Edition, GretagMacbeth, New Windsor, NY

Nable RO, Bañuelos GS, Paull JG (1997) Boron toxicity. Plant Soil 193:181–198

Narukawa T, Riley KW, French DH, Takatzu A, Chiba K (2003) Investigation into the relationship between major and minor element contents and particle size and leachability of boron in fly ash from coal fuel thermal power plants. J Environ Monit 5:831–836

Norgate T, Haque N (2012) Using life cycle assessment to evaluate some environmental impacts of gold production. J Clean Prod 29–30:53–63

North American Datum of 1983 (1989) In Schwarz CR (ed) NOAA professional paper 2, National Geodetic Survey (NGS), National Oceanic and Atmospheric Administration. U.S. Government Printing Office

Payne D (1992) Geochemistry of boron in selected gold deposits from the western United States. MS thesis, Eastern Washington Univ, Cheney, WA, USA

Senior LA, Sloto RA (2006) Arsenic, boron, and fluoride concentrations in ground water in and near diabase intrusions, Newark Basin, Southeastern Pensylvania. USGS SI Report 5261, Reston, VA, USA

Shibli A, Srebnik M (2005) Environmental aspects of boron. In: Abu Ali H (ed) Contemporary aspects of boron: Chemistry and biological applications, Studies Inorganic Chemistry 22:552–593

Paliewicz CC, Sirbescu, M-LC, van Hees EH, Sulatycky T (2012) Boron contamination at the McIntyre tailings, Timmins, Ontario. In: V.M. Goldschmidt Conference Abstract, Mineral Magazine 75: 2380

Slack JF (1996) Tourmaline associations with hydrothermal ore deposits. In: Grew ES, Anovitz LM (eds) Boron mineralogy, petrology, and geochemistry. Reviews mineralogy 33:559–664

Slack JF, Trumbull RB (2011) Tourmaline as a recorder of ore-forming processes. Elements 7:321–326

Smith GI, Medrano MD (1996) Continental borate deposits of Cenozoic age. In: Grew ES, Anovitz LM (eds) Boron mineralogy, petrology, and geochemistry. Reviews mineralogy 33:263-280

Stevens CJ, Sulatycky T, Small CA, Götz L, Taillefer RT, Burke LE (2013) Planning for closure—Porcupine Gold Mines' mine closure program. Accessed 3 Jan 2014 at https://circle.ubc.ca/bitstream/handle/2429/45306/Stevens_C_J_et_al_BC_Mine_2013.pdf?sequence=1

USEPA (2006) Boric Acid/Sodium Borate Salts: HED chapter of the tolerance reassessment eligibility decision document (TRED), Washington DC, USA

USEPA (US Environmental Protection Agency) (2008) Boron. Ch 3, Regulatory determinations support document for selected contaminants from CCL 2, EPA Report 815–R–08–012, Washington DC, USA

Walker CT (1975) Geochemistry of boron. Benchmark papers in geology volume 23, Wiley, Toronto, ON, Canada

Watanabe T (1975) Geochemical cycle and concentration of boron in the Earth's crust. In: Walker CT (ed) Geochemistry of boron, benchmark papers in geology 23. Wiley, Toronto, pp 167–178

Wentworth CK (1922) A scale of grade and class terms for clastic sediments. J Geol 30:377–392

WHO (2009) Boron in drinking water, background document for development of WHO guidelines for drinking-water quality. WHO Press, World Health Organization

Williams SJ, Arsenault MA, Buczkowski BJ, Reid JA, Flocks JG, Kulp MA, Penland S, Jenkins CJ (2006) Surficial sediment character of the Louisiana offshore continental shelf region: a GIS compilation, USGS Open File Report 2006–1195; accessed 03 Jan 2014 at http://pubs.usgs.gov/of/2006/1195/index.htm

Wolska J, Bryjak M (2013) Methods for boron removal from aqueous solutions–a review. Desalination 310:18–24

Yoshinaga J, Kida A, Nakasugi O (2011) Statistical approach for the source identification of boron in leachates from industrial landfills. J Mater Cycles Waste Manag 3:60–65